International Journal of Thermophysics, Vol. 22, No. 5, September 2001 (© 2001)

A Viscosity Equation of State for R123 in the Form of a Multilayer Feedforward Neural Network[1]

G. Scalabrin,[2,3] C. Corbetti,[2] and G. Cristofoli[2]

A *multilayer feedforward neural network* (MLFN) technique is adopted for developing a viscosity equation $\eta = \eta(T, \rho)$ for R123. The results obtained are very promising, with an average absolute deviation (AAD) of 1.02% for the currently available 169 primary data points, and are a significant improvement over those of a corresponding conventional equation in the literature. The method requires a high-accuracy equation of state for the fluid to be known to convert the experimental P, T into the independent variables ρ, T, but such equation may not be available for the target fluid. With a view to overcoming this difficulty, a viscosity implicit equation of state in the form of $T = T(P, \eta)$, avoiding the density variable, is obtained using the MLFN technique, starting from the same data sets as before. The prediction accuracy achieved is comparable with that of the former equation, $\eta = \eta(T, \rho)$.

KEY WORDS: 2,2-dichloro-1,1,1-trifluoroethane; feedforward neural networks; R123; viscosity correlation techniques; viscosity equation.

1. INTRODUCTION

The state of the art of viscosity surface representation, on which the present work focuses, suggests at least two approaches for its calculation. First, predictive or semipredictive models can be used. These models are often based on corresponding-states theory [1–4], and, in many cases, they are capable of estimating the property with an accuracy level sufficient for engineering calculations.

Alternatively, dedicated viscosity equations can be used which are based on the residual concept superimposing three parts: the dilute gas, the

[1] Paper presented at the Fourteenth Symposium on Thermophysical Properties, June 25–30, 2000, Boulder, Colorado, U.S.A.

[2] Dipartimento di Fisica Tecnica, Università di Padova, via Venezia 1, I-35131 Padova, Italy.

[3] To whom correspondence should be addressed. E-mail: gscala@unipd.it

0195-928X/01/0900-1383/0 © 2001 Plenum Publishing Corporation

excess terms, and the critical enhancement. This technique is essentially correlative and requires experimental data distributed as evenly as possible over the whole thermodynamic $P\rho T$ surface. Generally speaking, these equations are in the form $\eta = \eta(T, \rho)$, where η, T, and ρ are the viscosity, absolute temperature, and density, respectively. In conventional dedicated viscosity equation development, the coefficients are not obtained from direct experimental data regression. Since the viscosity data are inevitably related to the experimentally accessible (T, P) variables, an equation of state is needed to convert (T, P) into (T, ρ). Moreover, viscosity data at pressures approaching zero have to be extrapolated to fit the coefficients of the dilute-gas term in the viscosity equation. Because the final correlation relies only on the available data, this poses the question of whether a completely empirical correlation $\eta = \eta(T, \rho)$ could be developed directly from data alone.

The aim of the present work is to develop two viscosity equations, the first explicit and the second implicit in η, based directly on experimental data through a *multilayer feedforward neural network* (MLFN), which can be considered one of the most powerful and flexible regression techniques for function approximation.

The study is devoted to 2,2-dichloro-1,1,1-trifluoroethane (R123), for which a conventional dedicated viscosity equation has already been developed [5], thus enabling a comparison of the results. In addition, a large number of data is available for refrigerants.

2. DEDICATED VISCOSITY EQUATION

2.1. Conventional Technique

According to the residual viscosity concept [6], a viscosity correlation is expressed in the following form:

$$\eta(T, \rho) = \eta_0(T) + \Delta\eta_R(T, \rho) + \Delta\eta_c(T, \rho), \tag{1}$$

where $\eta_0(T)$ is the dilute-gas term representing the zero-density limit of the gas viscosity. Some theoretical guidance on the analytical form of this term can be derived from the kinetic theory of gases. This term has to be treated independently of the other two, the data required for regressing the coefficients are obtained at atmospheric pressure or below, and it is common to extrapolate such data to the zero-density limit.

$\Delta\eta_R(T, \rho)$ is the residual or excess function for the calculation of which the dilute gas and the critical enhancement terms must be subtracted from the actual viscosity value. Experience shows that third- or higher-order

polynomials of reduced density are often suitable forms for representing this term, disregarding temperature dependence, particularly when the database is limited. For polar fluids in the vapor phase, the quantity $(\partial\eta/\partial\rho)_T$ depends on the temperature and it is positive for higher T and negative for lower T. As a consequence, more complex analytical forms for the excess function are needed.

The critical enhancement term $\Delta\eta_c(T, \rho)$ describes the behavior of a fluid in the critical region, where the transport properties are influenced by long-range fluctuations. The critical enhancement of the transport properties can be described by a crossover theory [7, 8]. This term has only a modest influence on viscosity, and then only when very close to the critical point; it is consequently not taken into account in this work.

To calculate any $\eta = \eta(T, P)$ value, an equation of state is necessary for variable conversion. Considering how sensitive viscosity is to density in the dense phase, such an equation has to be very accurate.

2.2. Dedicated Viscosity Equations for R123

Tanaka and Sotani [5] developed a dedicated viscosity equation for R123 using the conventional procedure. To convert the (T, P) variables into (T, ρ), they adopted the MBWR-32 equation of state from Younglove and McLinden [9].

Tanaka and Sotani [5] regressed the dilute-gas function from data measured at atmospheric pressure. Because viscosity data under this condition are lacking, they generated further values by means of the Chapman–Enskog equation. In this way, they obtained a polynomial representation of $\eta_0(T)$. The critical enhancement term was neglected since no experimental data are available close to the critical point.

Regarding the excess term, $\Delta\eta_R(T, \rho)$ was split into two parts:

$$\Delta\eta_R(T, \rho) = \eta_1(T)\,\rho + \Delta_h\eta(\rho) \tag{2}$$

where $\eta_1(T)\,\rho$ takes into account the density dependence at low density values. This is a polynomial with coefficients fitted to vapor viscosity data. The term $\Delta_h\eta(\rho)$ is the high-density contribution, the form of which is a third-degree polynomial combined with a hyperbolic term. For the analytical forms and the coefficient values, reference can be made to the original article [5]. The validity ranges of the Tanaka and Sotani viscosity equation are $253 \leqslant T \leqslant 423$ K and $0 \leqslant \rho \leqslant 1608\ \mathrm{kg \cdot m^{-3}}$. According to the authors, the final equation gives an uncertainty of 1.17% for the primary data and 2.25% for the total data sets.

3. NEURAL NETWORKS

In the preceding sections it was pointed out that

(a) although the structure of the conventional viscosity equation sounds theoretically well-based, experimental data distributed over the whole $P\rho T$ surface are needed to regress the coefficients of the three contributions;

(b) it is by no means easy to find the most suitable analytical form for representing the density dependence of the residual term;

(c) the fitting procedure is not direct from the data, which have to be converted to split the influences of the three terms; and

(d) a highly accurate equation of state is needed for converting the measured variables (T, ρ) into (T, P).

Because experimental data covering the whole $P\rho T$ surface are needed for the development of a conventional viscosity equation dedicated to a target fluid, it seems reasonable to test a single correlative technique based directly on all the available data. Clearly, the analytical form of the new model has to prove highly flexible in fitting the experimental viscosity surface of a generic fluid. The optimal characteristics expected for this form are (a) an *a priori* known form and (b) a unique and suitable form for a larger number of target fluids. It was established during the preliminary stages that neural networks, applied as function approximators, have demonstrated the required characteristics to a high degree.

A new correlation technique is proposed here, based on neural networks. The heart of the problem is to fit such a correlation on the available viscosity data for developing a neural network viscosity equation. Among neural network architectures, the MLFN with only one hidden layer seems to be the most effective as a universal approximator of continuous functions in a compact domain [10–12]. In this architecture there are several neuron layers (*multilayer*) and the information goes in only one direction, from input to output (*feedforward*), i.e., from left to right in Fig. 1. This figure shows the general architecture of a MLFN with a hidden layer, which is the analytical tool used in the present work as a viscosity equation model.

The $I-1$ inputs U_i enter the $I-1$ neurons of the input layer. The inputs U_i represent the independent variables of the problem. The input information is not manipulated by the input layer neurons; it is only transmitted. The last neuron, at the number I, receives Bias 1. The J neurons of the hidden layer receive the weighted sum of signals from the input layer. A nonlinear transfer function is applied to this sum. The

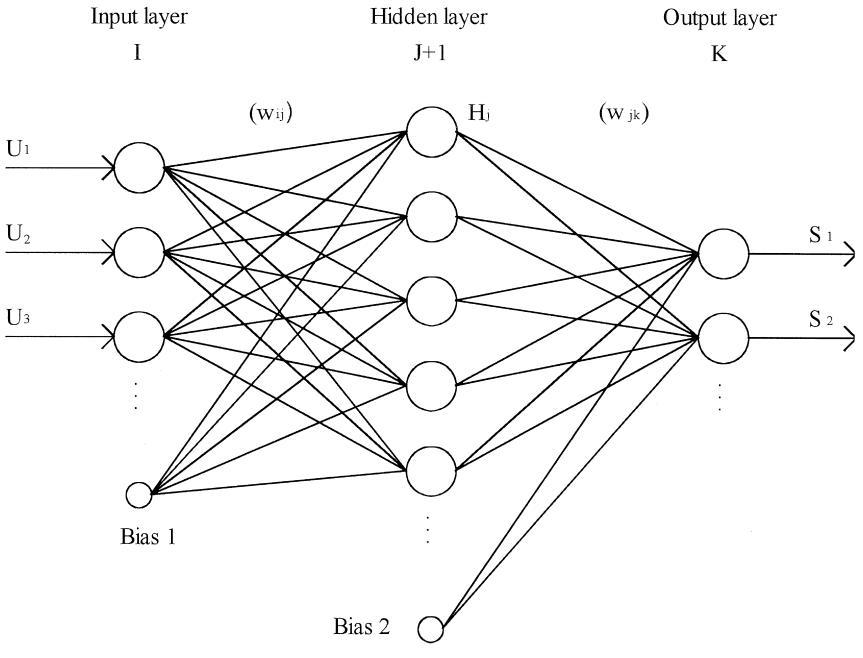

Fig. 1. General architecture of a *multilayer feedforward network*.

neuron number $J+1$ receives only the bias value. If H_j is the output of the j hidden layer, this is

$$H_j = f\left(\sum_{i=1}^{I} w_{ij}U_i\right), \qquad 1 \leqslant j \leqslant J \tag{3}$$

$$H_{J+1} = \text{Bias 2} \tag{4}$$

where f is the transfer function and w_{ij} are the weighting factors. Finally, the K neurons of the output layer receive the weighted sum of signals from the hidden layer and, once again, apply a nonlinear transfer function to the sum. The outputs S_k represent the dependent variables of the problem. If S_k is the output of the output layer, i.e., the final output of the MLFN, this is

$$S_k = f\left(\sum_{j=1}^{J+1} w_{jk}H_j\right), \qquad 1 \leqslant k \leqslant K \tag{5}$$

Though the architecture is fixed, the MLFN is very flexible because both the number of neurons in the hidden layer J and the form of the

transfer function f can be chosen. The input I and the output K neuron numbers depend on the kind of problem to be solved. In addition, the two matrices of the weighting factor, $w_{ij}[I \times J]$ and $w_{jk}[(J+1) \times K]$, have to be defined case by case. When J and f have been chosen, the weighting factors can be fitted on some sets of known outputs. This regression step is called a *training* step. Bias 1 and Bias 2 are two constants able to make the convergence easier and faster during fitting.

Some criteria have to be kept in mind in the choice of the transfer function f. This has to be a continuous and derivable function, and it has to be limited. The choice of the analytical form of f does not affect the performance of the MLFN (which depends strictly on the weighting factors w_{ij} and w_{jk}), but it does affect the training procedure. The transfer function used in the present work has a sigmoid form:

$$f(x) = \alpha \frac{1}{1+e^{-2\beta x}} \tag{6}$$

Two positive parameters have been applied in Eq. (6) to make the function's behavior more flexible: α changes the activation span and β determines the steepness of the sigmoid function. As a consequence of the choice of a transfer function, Eq. (6), $S_k \leqslant \alpha$ for every $k = 1, K$. In addition, the training step is easier if all the inputs are of the same magnitude. That is why both input and output values are compressed here within the same range by Eqs. (7)–(10) and (13).

The analytical form of the present MLFN is

$$f(x) = \alpha \frac{1}{1+e^{-2\beta x}} \tag{6}$$

$$g(x) = \ln(x+1) \tag{7}$$

$$u_i = \frac{A_{\max} - A_{\min}}{V_{\max,\,i} - V_{\min,\,i}}, \qquad 1 \leqslant i \leqslant I-1 \tag{8}$$

$$s_k = \frac{A_{\max} - A_{\min}}{g(W_{\max,\,k}) - g(W_{\min,\,k})}, \qquad 1 \leqslant k \leqslant K \tag{9}$$

$$W_k = \exp\left[\frac{S_k - A_{\min}}{s_k} + g(W_{\min,\,k})\right] - 1, \qquad 1 \leqslant k \leqslant K \tag{10}$$

$$S_k = f\left(\sum_{j=1}^{J+1} w_{jk} H_j\right), \qquad 1 \leqslant k \leqslant K \tag{11}$$

$$H_j = f\left(\sum_{i=1}^{I} w_{ij} U_i\right), \qquad 1 \leqslant j \leqslant J \tag{12}$$

$$H_{J+1} = \text{Bias } 2$$

$$U_i = u_i(V_i - V_{\min,i}) + A_{\min}, \qquad 1 \leqslant i \leqslant I-1 \tag{13}$$

$$U_I = \text{Bias } 1$$

where J is the number of neurons in the hidden layer, $A_{\min}$ and $A_{\max}$ are the allowable range limits of the compressed input variables, $V_{\min,i}$ and $V_{\max,i}$ are the limits of the independent input variables for the training set, and $W_{\min,k}$ and $W_{\max,k}$ are the limit values of the output functions. The quantity V_i is the independent variable, and W_k is the dependent variable. Due to the characteristics of the present problem, the MLFN parameters are set here to the following values:

$$I = 3, \qquad \text{Bias } 1 = 1.0, \qquad A_{\min} = 0.05, \qquad \alpha = 1.0$$

$$K = 1, \qquad \text{Bias } 2 = 1.0, \qquad A_{\max} = 0.95, \qquad \beta = 0.005$$

In this way the input variables and the output function have both been compressed in the range 0.05 to 0.95. To complete the MLFN definition, the following parameters have to be calculated for each target fluid through a training step: J, $V_{\min,i}$, $V_{\max,i}$, $W_{\min,k}$, $W_{\max,k}$, w_{ij}, and w_{jk}. Since the MLFN architecture is always the same, its connotative contents are in general the number of hidden layers, the number of nodes, and the matrixes of weighting factors w_{ij} and w_{jk}. It has been established that a single hidden layer suffices for representing a continuous function. The number J of neurons in the hidden layer has to be found by subsequent trials; this number has to minimize the residual error during the training procedure. In addition, for each number of hidden layer nodes, two matrixes, w_{ij} and w_{jk}, of coefficients have to be found. Determining the optimum number of hidden nodes and fitting the two matrixes w_{ij}, w_{jk} are part of the training procedure.

Given an experimental data set of output S_k, in the independent variables U_i, the weighting factors are found by minimizing the following objective function by means of an optimization procedure.

$$f_{\text{ob}} = \frac{1}{K} \sum_{k=1}^{K} (S_k^{\text{calc}} - S_k^{\text{exp}})^2 \tag{14}$$

As in any optimization process, the optimized parameter set must not depend on the algorithm assumed and several methods have to be tested for the same equivalent result.

4. VISCOSITY NEURAL NETWORK EQUATIONS

Since an MLFN is a mathematical function that links some inputs with some outputs, it seems reasonable to correlate viscosity data with the independent variables using this technique. To verify the approximating capability of an MLFN regarding a viscosity equation, as a preliminary test we generated viscosity data from the Tanaka–Sotani equation [5] and trained the neural network on those data.

In our case, Eqs. (6)–(13), considering that $I = 3$ and $K = 1$, it becomes

$$V_1 = T_r, \qquad V_2 = \rho_r, \qquad W_1 = \eta_r \tag{15}$$

where the reducing critical parameters are $T_c = 456.831$ K, $P_c = 3.6618$ MPa, and $\rho_c = 550\ \mathrm{kg \cdot m^{-3}}$. The viscosity reducing factor is $H_c = (M^{1/2} P_c^{2/3} / R^{1/6} N_A^{1/3} T_c^{1/6}) = 27.8509\ \mu\mathrm{Pa \cdot s}$ where M is the molecular mass, R is the universal gas constant, and N_A is the Avogadro number.

The viscosity data generated amounted to 3674 points; 460 were used in the training step and the remainder for validating the MLFN equation obtained. The generated data enabled a regression of the parameters of the neural network. With reference to the previous paragraph, the optimum number of neurons in the hidden layer in this case is $J = 10$. The weighting factors are 30 for the first matrix, w_{ij}, and 11 for the second matrix w_{jk}, for a total of 41 weighting factors. The values of the weighting factor (w_{ij} and w_{jk}) matrixes are the fluid specific MLFN viscosity parameters.

Of the generated data, 3214 were used for validating the equation, which resulted in an average absolute deviation (AAD) of 0.096%, a bias of 0.003%, and a maximum deviation of 0.94%. These results suggest that the MLFN is a very valuable tool for fitting a viscosity surface.

The data are generally classified as *primary* or *secondary*, and only the former are used in the correlation regression. The guidelines for the screening procedure are discussed in specialized textbooks, e.g., Ref. 6. In the present work, due partly to the paucity of the R123 experimental data available, the screening procedure adopted was as follows. We maintained as primary the data considered by Tanaka and Sotani as primary in developing their equation, even if they were measured at temperatures and pressures outside the validity range of their equation. We tested all available experimental viscosity data versus the dedicated Tanaka–Sotani equation and included all data with deviations of less than 6%. We also included data that were

not considered by Tanaka and Sotani, such as the data provided by Mayinger [17]. The data screened in this way were considered *primitive*. Using these data, a first neural network version was regressed. After this preliminary screening the first neural network was tested versus the primitive data. Avoiding the experimental points with deviations higher than 2%, a finer screening was done to identify the primary data, amounting to 169 in all, over which the final viscosity MLFN equation was fitted.

After the data screening, the weighting factors of the MLFN equation—which are the new viscosity equation parameters for R123 in the general form $\eta = \eta(T, \rho)$—can be obtained. In addition to considering a viscosity equation of the previous form,

$$\eta = \eta(T, \rho) \tag{16}$$

which has to be coupled with an equation of state for variable conversion, an equation system such as the one below could be written [13]:

$$\begin{cases} \eta = \eta(T, \rho) \\ P = P(T, \rho) \end{cases} \tag{17}$$

From this system a functional form $F(P, T, \eta) = 0$ could be derived, avoiding density as a variable and consequently not requiring the use of a high-accuracy equation of state for the target fluid. From such an F form, we propose extracting the functional form,

$$T = T(P, \eta) \tag{18}$$

by means of the former MLFN technique, always based exclusively on the experimental data. The other possible form $P = P(T, \eta)$ has been discarded due to the higher difficulty of training the MLFN, while the form $\eta = \eta(T, P)$ cannot be considered for the whole surface, because at saturation for a given T, $P^S(T)$ input couple, i.e., temperature, the two viscosity values η^S_{liq}, η^S_{vap} have to be output. The new functional form, Eq. (18), is called here the *viscosity equation of state* because it merges a viscosity equation and a thermodynamic equation of state.

Following the preceding procedure the two proposed MLFNs have been obtained and their parameters are listed in Table I. For the viscosity explicit equation $V_1 = T_r$, $V_2 = \rho_r$, and $W_1 = \eta_r$, while for the temperature explicit equation $V_1 = P_r$, $V_2 = \eta_r$, and $W_1 = T_r$. In the latter case the filter function $g(x)$, Eq. (7), is applied to V_2 instead of W_1.

The validity ranges for both new viscosity equations are $170 \leqslant T \leqslant 423$ K, $4.5 \leqslant \rho \leqslant 1760$ kg·m^{-3}, and $7 \times 10^{-6} \leqslant P \leqslant 34$ Mpa.

Table I. Parameters for the Two MLFN Viscosity Equations

Viscosity explicit MLFN eq.: $\eta_r = \eta_r(T_r, \rho_r)$						Temperature explicit MLFN eq.: $T_r = T_r(P_r, \eta_r)$					
i	j	w_{ij}	j	k	w_{jk}	i	j	w_{ij}	j	k	w_{jk}
1	1	0.1500632×10^{4}	1	1	-0.1691426×10^{4}	1	1	0.6440240×10^{3}	1	1	0.1712521×10^{4}
2	1	-0.2908013×10^{4}	2	1	0.3059703×10^{4}	2	1	-0.3410896×10^{4}	2	1	0.7175858×10^{4}
3	1	0.2964611×10^{4}	3	1	0.5545804×10^{3}	3	1	0.5974824×10^{3}	3	1	-0.5253422×10^{4}
1	2	-0.5308147×10^{2}	4	1	0.1245187×10^{4}	1	2	-0.4088969×10^{4}	4	1	-0.5870102×10^{4}
2	2	0.1294263×10^{4}	5	1	-0.1486148×10^{4}	2	2	0.7838231×10^{4}	5	1	-0.5929326×10^{4}
3	2	-0.1516965×10^{4}	6	1	0.1893007×10^{4}	3	2	0.2326999×10^{3}	6	1	-0.2490978×10^{4}
1	3	0.1105456×10^{3}	7	1	0.2026413×10^{4}	1	3	0.1124305×10^{4}	7	1	0.1225327×10^{4}
2	3	-0.4978172×10^{3}				2	3	-0.8897859×10^{4}			
3	3	-0.1607605×10^{2}				3	3	0.5676846×10^{3}			
1	4	-0.1836850×10^{2}				1	4	-0.1773198×10^{2}			
2	4	0.3303200×10^{3}				2	4	0.2951690×10^{3}			
3	4	-0.3956871×10^{2}				3	4	-0.5794737×10^{3}			
1	5	0.6168072×10^{3}				1	5	-0.3993590×10^{2}			
2	5	-0.1511499×10^{4}				2	5	0.5533852×10^{3}			
3	5	0.1912588×10^{4}				3	5	0.1400350×10^{3}			
1	6	-0.6117513×10^{2}				1	6	-0.2392280×10^{4}			
2	6	-0.1349390×10^{4}				2	6	0.1304965×10^{5}			
3	6	-0.2979162×10^{3}				3	6	-0.6789685×10^{3}			

$V_{\min,1} \equiv T_r^{\min}$	0.372128862	$V_{\min,1} \equiv P_r^{\min}$	2.02142×10^{-6}
$V_{\max,1} \equiv T_r^{\max}$	0.926272517	$V_{\max,1} \equiv P_r^{\max}$	9.17854607
$V_{\min,2} \equiv \rho_r^{\min}$	0.008196364	$V_{\min,2} \equiv \eta_r^{\min}$	0.399160894
$V_{\max,2} \equiv \rho_r^{\max}$	3.203118255	$V_{\max,2} \equiv \eta_r^{\max}$	200.6755631
$W_{\max,1} \equiv \eta_r^{\min}$	0.399160894	$W_{\min,1} \equiv T_r^{\min}$	0.372128862
$W_{\max,1} \equiv \eta_r^{\max}$	200.6755631	$W_{\max,1} \equiv T_r^{\max}$	0.926272517
J	6	J	6
Training residual AAD%	1.02	Training residual AAD% (T_r)	0.383

Table II. Validation Results of the Viscosity Explicit MLFN, Eq. (16), and Temperature Explicit MLFN, Eq. (18), and of the Tanaka–Sotani Dedicated Equation [5]

			Viscosity explicit MLFN, Eq. (16)			Temp. explicit MLFN, Eq. (18)			Viscosity dedicated equation from Tanaka–Sotani					
Phase	Range, T (K)	Range, P (MPa)	AAD (%)	Bias (%)	Max (%)	AAD (%)	Bias (%)	Max (%)	AAD (%)	Bias (%)	Max (%)	NPT	Method[a]	Ref. No.
						Primary data								
L	200–300	3.2–33..6	1.91	−1.79	4.46	1.85	−1.81	4.57	6.09(1.77)	−6.05(−1.64)	14.46(3.66)	29(9)	TC	14[b]
SL	170–320	—	1.12	−0.17	3.74	1.31	0.09	3.84	5.87(1.77)	−5.85(−1.73)	25.21(5.15)	23(4)	TC	14[b]
V	308–363	0.1	1.03	1.03	1.75	0.91	0.51	1.42	0.69	0.47	1.77	4	CV	15
SL	273–353	—	0.70	−0.11	1.72	0.37	0.29	0.69	1.68	−1.68	4.42	9	CV	16
L	233–418	1.1–20.7	1.02	0.94	3.83	1.33	0.86	4.06	1.89(1.52)	−0.31(0.28)	5.59(4.76)	64(54)	CV	19[b]
V	323–423	0.13–2.0	0.43	−0.09	0.91	0.40	−0.02	1.96	0.24	−0.09	0.82	42	OD	22
Avg.			1.02	0.01	4.46	1.12	0.04	4.57	2.70(1.14)	−2.05(−0.31)	25.21(5.15)	169(132)[c]		
						Secondary data								
SC	473–523	4.0–7.0	4.26(—)	−3.35(—)	14.14(—)	—(—)	—(—)	—(—)	4.63(—)	−4.63(—)	6.65(—)	25(0)	OD	17[b]
V	303–523	0.1–3.5	2.14(2.08)	−0.75(−1.97)	9.30(7.00)	—(1.96)	—(−1.92)	—(8.32)	3.05(1.93)	−3.05(−1.93)	7.17(5.92)	244(80)	OD	17[b]
SV	303–443	—	366(2.82)	−3.00(−2.07)	10.00(6.62)	—(2.16)	—(−1.98)	—(8.51)	2.38(1.94)	−2.37(−1.92)	7.23(4.83)	15(13)	OD	17[b]
V	303–423	0.1–2.0	1.75	−1.26	8.87	1.46	−1.27	10.32	1.51	−1.51	7.49	31	OD	18
L	293	0.1	3.09	3.09	3.09	3.05	3.05	3.05	2.25	2.25	2.25	1	PCS	20
SV	—	0.1–2.5	3.70(3.36)	−3.26(−2.90)	8.30(7.21)	—(3.08)	—(−2.70)	—(8.80)	2.76(2.57)	−2.75(−2.56)	5.61(5.61)	15(14)	OD	17[b]
V	323–423	0.13–2.0	2.43	−2.38	8.55	2.37	−2.34	9.65	2.99	−2.99	7.73	47	C	21
Avg.			2.41	−1.34(−2.01)	14.14(8.87)	2.12	−1.95	10.32	2.98(2.18)	−2.97(−2.15)	7.73(7.73)	378(186)[c]		
Overall			1.98(1.67)	−0.92(−1.05)	14.14(8.87)	1.64	−1.00	10.32	2.89(1.75)	−2.68(−1.39)	25.21(5.92)	547		

[a] CV, capillary viscometer; TC, torsionally oscillating quartz crystal viscometer; OD, oscillating disk viscometer; PCS, photon correlation spectroscopy; C, calculated [21].

[b] For such references the numbers in parentheses refer to experimental points falling inside the validity ranges of equations.

[c] For the Tanaka–Sotani equation, 132 primary and 186 secondary data are in the validity range, while for the MLFN, Eq. (16) and Eq. (18), all 169 primary data and 186 secondary data are in the validity range.

The validation of the two new viscosity equations is reported in Table II, together with comparison with the Tanaka–Sotani dedicated equation. The data are split into primary and secondary sets as discussed previously. The primary set has been used for the training step, and consequently, the corresponding AADs are to be considered the residual errors of the correlations. Regarding the temperature explicit equation, the training residual AAD (Table I) refers to the temperature, which is the dependent variable. In Table II the AAD is calculated for viscosity values. Some further references are cited in the work of Tanaka and Sotani, but they considered them as secondary sources. In addition, we have not found those references, and consequently we have neglected the related data. Between data from Mayinger and Nabizadeh [17, 18] and data from Takahashi and Yokoyama [21, 22], a discrepancy of between 3.5 and 8.25% was found at pressures higher than 1 MPa in the vapor phase and the reason may be the kind of viscometer used. Consequently, the sources [17, 18] have been considered secondary.

5. CONCLUSIONS

A new method has been proposed for the development of a dedicated viscosity equation and has been applied to refrigerant R123, for which a former conventional dedicated equation was available. The new method is based on the *multilayer feedforward network* technique, which has been demonstrated to be a powerful and flexible universal function approximator and has been able to reproduce with high accuracy the viscosity surface of the former conventional equation. The method is completely correlative and based directly on the available viscosity data. Two viscosity functions are proposed here: the first is viscosity explicit, $\eta = \eta(T, \rho)$, and the other is temperature explicit, $T = T(P, \eta)$, and does not require a high accuracy equation of state for the variable conversion. The validity ranges of both equations are $170 \leqslant T \leqslant 423$ K, $4.5 \leqslant \rho \leqslant 1760$ kg·m^{-3}, and $7 \times 10^{-6} \leqslant P \leqslant 34$ MPa, which correspond to the primary data boundaries. The obtained accuracy on primary data for both equations is in the AAD range of 1 to 1.1%, which is a significant improvement with respect to the conventional equation. This work shows that neural networks are promising tools for transport property equation development.

REFERENCES

1. K. J. Okeson and R. L. Rowley, *Int. J. Thermophys.* **12**:119 (1991).
2. G. Scalabrin and M. Grigiante, Presented at 13th Symp. Thermophys. Prop. (Boulder, CO, 1997).

3. G. Cristofoli, M. Grigiante, and G. Scalabrin, *High Temp. High Press.* **33**:83 (2001).
4. M. McLinden, *NIST Database 23, Version 5.0 (REFPROP)* (Natl. Inst. Stand. Technol., Boulder, CO, 1995).
5. Y. Tanaka and T. Sotani, *Int. J. Thermophys.* **17**:293 (1996).
6. J. Millat, J. H. Dymond, and C. A. Nieto de Castro, *Transport Properties of Fluids* (Cambridge University Press, Cambridge, UK, 1996).
7. G. A. Olchowy and J. V. Sengers, *Phys. Rev. Lett.* **61**:15 (1988).
8. J. Luettmer-Strathmann, J. V. Sengers, and G. Olchowy, *J. Chem. Phys.* **103**:7482 (1995).
9. B. A. Younglove and M. O. McLinden, *J. Phys. Chem. Ref. Data* **23**:731 (1994).
10. G. Cybenko, *Math. Control Signals Syst.* **2**:303 (1989).
11. K. Hornik, M. Stinchcombe, and H. White, *Neural Networks* **2**:359 (1989).
12. V. Kurkova, *Neural Networks* **5**:501 (1992).
13. A. Laesecke, R. Krauss, K. Stephan, and W. Wagner, *J. Phys. Chem. Ref. Data* **19**:1089 (1990).
14. D. E. Diller, A. S. Aragon, and A. Laesecke, *Fluid Phase Equil.* **88**:251 (1993).
15. D. C. Dowdell and G. P. Matthews, *J. Chem. Soc. Faraday. Trans.* **89**:3545 (1993).
16. A. Kumagai and S. Takahashi, *Int. J. Thermophys.* **12**:105 (1991).
17. F. Mayinger, DFG-Forschungsvorhaben, Abschlußbericht (1991).
18. H. Nabizadeh and F. Mayinger, *High Temp. High Press* **24**:221 (1992).
19. T. Okubo and A. Nagashima, *Int. J. Thermophys.* **13**:401 (1992).
20. S. Will and A. Leipertz; *Int. J. Thermophys.* **16**:433 (1995).
21. M. Takahashi, C. Yokoyama, and S. Takahashi, *Proc. 11th Japan Symp. Thermophys. Prop.* (1990), pp. 115–118.
22. C. Yokoyama and M. Takahashi, *Int. J. Thermophys.* **21**:695 (2000).